PHYSICAL REVIEW D **88,** 084046 (2013)

Loaded magnetohydrodynamic flows in Kerr spacetime

Noemie Globus and Amir Levinson
School of Physics and Astronomy, Tel Aviv University, Tel Aviv 69978, Israel
(Received 27 August 2013; published 25 October 2013)

The effect of mass and energy loading on the efficiency at which energy can be extracted magnetically from a Kerr black hole is explored, using a semianalytic, ideal magnetohydrodynamics model that incorporates plasma injection on magnetic field lines. We find a critical load below which the specific energy of the plasma inflowing into the black hole is negative, and above which it is positive, and identify two types of flows with distinct properties; at subcritical loads a magnetic outflow is launched from the ergosphere, owing to extraction of the black hole spin energy, as originally proposed by Blandford and Znajek. At supercritical loads the structure of the flow depends on the details of the injection process. In cases where the injected plasma is relativistically hot, a pressure-driven, double transmagnetosonic flow is launched from a stagnation point located outside the ergosphere, between the inner and outer light cylinders. Some fraction of the energy deposited in the magnetosphere is then absorbed by the black hole and the rest emerges at infinity in the form of a relativistic outflow. When the injected plasma is cold an outflow may not form at all. We discuss the implications of our results to gamma ray bursts and active galactic nuclei.

DOI: 10.1103/PhysRevD.88.084046 PACS numbers: 04.70.−s, 47.75.+f, 95.30.Qd

I. INTRODUCTION

A plausible production mechanism for the relativistic outflows observed in active galactic nuclei (AGNs), gamma ray bursts (GRBs), and microquasars is magnetic extraction of the spin energy of a Kerr black hole. It has been shown [1] that in the force-free limit, at which the inertia of the plasma is negligible, frame dragging induces an outward flow of energy along magnetic field lines threading the horizon, at the expense of the black hole's rotational energy. It is commonly thought that this outward energy flux ultimately transforms into a collimated relativistic jet, like those seen in the compact relativistic systems mentioned above. Indeed, recent numerical simulations (e.g., [2–7]) indicate that powerful outflows can be produced by this mechanism if sufficiently large magnetic flux can be accumulated near the horizon of the black hole.

A question of interest is how the inertia of the plasma injected on magnetic field lines affects the properties of the emerging outflow, and in particular what are the requirements for the activation of the Blandford-Znajek mechanism (hereafter BZ). Takahashi *et al.* [8] considered the structure of a cold magnetohydrodynamics (MHD) inflow in Kerr spacetime, and have shown that two conditions must be fulfilled in order for energy to be extracted: (i) the angular velocity of magnetic field lines must satisfy $0 < \Omega_F < \Omega_H$, where Ω_H is the angular velocity of the black hole, and (ii) the Alfvén point must be located inside the ergosphere. Condition (ii) is automatically satisfied in the force-free limit, but not necessarily in general. The question of how the location of the Alfvén point depends on the load was not addressed in [8].

In this paper we show that there is a critical energy load below which the outflow is powered by the black hole, and above which it is either powered by the external energy source or does not form at all. This critical load depends on the strength of magnetic field lines threading the horizon and the angular momentum of the black hole. One immediate consequence is that the mass inflow that supports the magnetic field near the horizon must be strongly suppressed in the polar region in order for a BZ outflow to be launched. A similar conclusion was drawn by Komissarov and Barkov [7], who conducted numerical experiments to study the effect of mass loading on the energy extraction process in GRBs. They have shown that in the collapsar model the requirement for the activation of the BZ process imposes stringent constraints on the progenitor star. But even if the progenitor accommodates those requirements and the polar region is devoid of baryons, substantial loading is anticipated owing to deposition of hot plasma by annihilation of neutrinos emanating from the accretion flow surrounding the black hole [9–12]. Below we show that if the inward enthalpy flux of the hot plasma deposited in the magnetosphere exceeds a certain value, the BZ process completely shuts down, and the outflow is powered by the neutrino source.

The relatively sensitive dependence of the activation condition on the angular momentum of the hole, derived in Sec. IV, suggests that outflows from slowly rotating black holes may be underpowered. This may explain the claimed radio loud and quiet dichotomy in AGNs [13], as discussed in some greater detail at the end of Sec. V.

II. A MODEL FOR IDEAL MHD FLOW WITH PLASMA INJECTION

The strong gravitational field of the black hole imposes an inward motion of plasma very near the horizon,

 © 2013 American Physical Society

regardless of the direction of the energy flux. On the other hand, under the conditions suitable for formation of a MHD outflow, the plasma above the outer light cylinder must be flowing outwards. Consequently, the particle flux flowing along magnetic field lines threading the ergosphere must always reverse its direction in the region located between the inner and outer light cylinders [14]. Hence, a complete treatment of MHD outflows in Kerr geometry requires proper account of plasma injection in the magnetosphere. In principle, one can envisage situations in which an outflow cannot be launched in the first place. For instance, dumping large amounts of mass at some arbitrary radius above the black hole, e.g., fallback matter from a stellar envelope in collapsars, will disable activation of the BZ process, giving rise to formation of a quasisteady accretion shock [7]. Such situations are not considered in what follows. Rather, we focus on cases where the system adjusts to sustain a steady, continuous flow. The model constructed below incorporates, in a self-consistent manner, a prescribed plasma source in the flow, as illustrated in Fig. 1. This source may be associated with mass injection on magnetic field lines, or pair production via annihilation of gamma rays in AGNs and microquasars (e.g., [15]), and neutrinos in GRBs [10,12], that emanate from the surrounding accretion disk. While the latter injection processes are well understood and can be accurately modeled, the process of mass injection is only poorly understood. Mass loading in GRB outflows may conceivably occur via leaking of free neutrons from the hot matter surrounding the jet [16], instabilities at the jet interface, or pickup of baryons from the inner disk. The last two processes may also be relevant to AGNs and microquasars. As described below, the MHD equations can be reduced to a system of equations governing the changes in mass, energy and angular momentum fluxes in terms of the corresponding source terms. The steady double flow emanating from the stagnation point (see Fig. 1) must pass smoothly through the inner and outer fast-and-slow magnetosonic points, the locations of which depend, quite generally, on the energy and momentum deposition profiles.

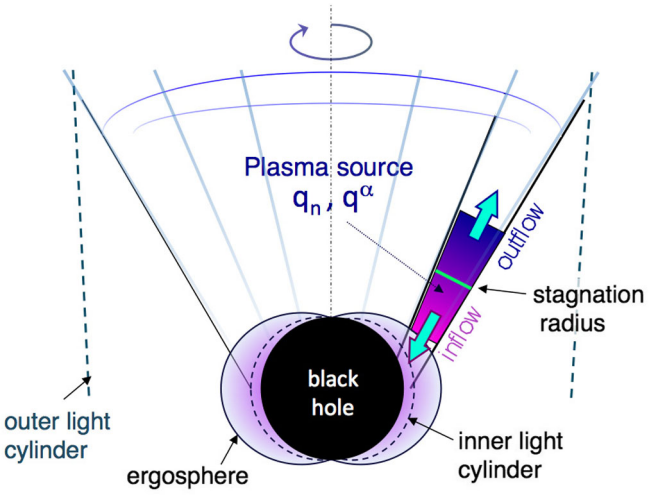

FIG. 1 (color online). A sketch of the flow structure along a particular streamline: A double transmagnetosonic, plasma flow is launched from a stagnation radius located between the inner and outer light cylinders. The lost plasma is replenished by an external plasma source, as indicated. At sufficiently small injection rates, the specific energy of the inflowing plasma is negative, whereas that of the outflowing plasma is positive, implying an outward flow of energy from the horizon to infinity. This type of flow is powered by the black hole spin energy. At high injection rates the specific energy is positive everywhere, implying a sign change of the energy flux and the toroidal magnetic field across the stagnation point. This type of flow is powered entirely by the external plasma source, with some fraction of the injected energy being absorbed by the black hole and the rest used to accelerate the outflow.

A. Basic equations

The stress-energy tensor of a magnetized perfect fluid takes the form

$$T^{\alpha\beta} = \bar{h}\rho c^2 u^\alpha u^\beta + p g^{\alpha\beta} + \frac{1}{4\pi}\left(F^{\alpha\gamma}F^{\beta}_{\gamma} - \frac{1}{4}g^{\alpha\beta}F^2\right), \tag{1}$$

where u^α is the 4-velocity measured in units of c, $\bar{h} = (\rho c^2 + e_{\rm int} + p)/\rho c^2$ the dimensionless specific enthalpy, ρ the baryonic rest-mass density, p the pressure, and $g_{\mu\nu}$ the coefficients of the metric tensor of the Kerr spacetime. In the following we use geometrical units ($c = G = 1$), unless otherwise stated, and express the Kerr metric in the regular Boyer-Lindquist coordinates:

$$\begin{aligned} ds^2 &\equiv g_{\mu\nu}dx^\mu dx^\nu \\ &= -\alpha^2 dt^2 + g_{\varphi\varphi}(d\varphi - \omega dt)^2 + g_{rr}dr^2 + g_{\theta\theta}d\theta^2, \end{aligned} \tag{2}$$

where the metric coefficients can be expressed as $g_{rr} = \Sigma/\Delta$, $g_{\theta\theta} = \Sigma$, and $g_{\varphi\varphi} \equiv \varpi^2 = A\sin^2\theta/\Sigma$, in terms of $\Delta = r^2 + a^2 - 2mr$, $\Sigma = r^2 + a^2\cos^2\theta$, and $A = (r^2 + a^2)^2 - a^2\Delta\sin^2\theta$. The parameters m and a are the mass and specific angular momentum per unit mass of the hole, respectively, with $m \geq |a|$. The coefficients $\alpha = \sqrt{\Sigma\Delta/A}$ and $\omega = 2mra/A$ measure, respectively, the time lapse and the frame dragging potential between a zero-angular-momentum observer (ZAMO) and an observer at infinity. The angular velocity of the black hole is defined as the value of ω on the horizon, viz., $\Omega_H \equiv \omega(r = r_H) = a/(2mr_H)$, where $r_H = m + \sqrt{m^2 - a^2}$ is the radius of the horizon, obtained from the condition $\Delta_H = 0$.

The dynamics of the flow is governed by the energy-momentum equations:

$$\frac{1}{\sqrt{-g}}(\sqrt{-g}T^{\alpha\beta})_{,\alpha} + \Gamma^{\beta}{}_{\mu\nu}T^{\mu\nu} = q^{\beta}, \tag{3}$$

mass conservation:

$$\frac{1}{\sqrt{-g}}\partial_{\alpha}(\sqrt{-g}\rho u^{\alpha}) = q_n, \tag{4}$$

and Maxwell's equations:

$$F^{\beta\alpha}_{\ ;\alpha} = \frac{1}{\sqrt{-g}}(\sqrt{-g}F^{\beta\alpha})_{,\alpha} = 4\pi j^{\beta}, \tag{5}$$

$$F_{\alpha\beta,\gamma} + F_{\beta\gamma,\alpha} + F_{\gamma\alpha,\beta} = 0. \tag{6}$$

Here, q^{β} denotes the source terms associated with energy-momentum transfer by an external agent, q_n is a particle source, and $\Gamma^{\beta}_{\mu\nu}$ denotes the affine connection. The magnetic field components measured by a ZAMO are given by $B_r = F_{\theta\varphi}/\sqrt{A}\sin\theta$, $B_\theta = \sqrt{\Delta}F_{\varphi r}/\sqrt{A}\sin\theta$ and $B_\varphi = \sqrt{\Delta}F_{r\theta}/\Sigma$ [17]. To simplify the notation we find it useful to define a redshifted poloidal magnetic field: $B_p = (B_r^2 + B_\theta^2)^{1/2}/\alpha$.

We consider a stationary and axisymmetric MHD flow in the limit of infinite conductivity, $F_{\alpha\beta}u^{\beta} = 0$. In general, the flow is characterized by a stream function $\Psi(r,\theta)$ that defines the geometry of magnetic flux surfaces, and by the following functionals of Ψ: the angular velocity of magnetic field lines $\Omega(\Psi)$, the ratio of mass and magnetic fluxes $\eta(\Psi)$, and the energy, angular momentum and entropy per baryon, denoted by $\mathcal{E}(\Psi)$, $\mathcal{L}(\Psi)$ and $s(\Psi)$, respectively. These quantities can be expressed in terms of the poloidal velocity, $u_p = \pm(u_r u^r + u_\theta u^\theta)^{1/2}$, where the plus sign applies to outflow lines and the minus sign to inflow lines, the redshifted poloidal magnetic field B_p, and the azimuthal magnetic field B_φ as [18–20]

$$\eta(\Psi) = \frac{\rho u_p}{B_p}, \tag{7}$$

$$\Omega_F(\Psi) = v^{\varphi} - \frac{v_p B_\varphi}{\varpi B_p}, \tag{8}$$

$$\mathcal{E}(\Psi) = -\bar{h}u_t - \frac{\alpha\varpi\Omega_F}{4\pi\eta}B_\varphi, \tag{9}$$

$$\mathcal{L}(\Psi) = \bar{h}u_\varphi - \frac{\alpha\varpi B_\varphi}{4\pi\eta}. \tag{10}$$

In Eq. (8) $v^{\varphi} = u^{\varphi}/u^t$ and $v_p = u_p/\gamma$, with $\gamma = u^t\alpha$ being the Lorentz factor measured by a ZAMO. Note that with our sign convention the value of η is positive on outflow lines and negative on inflow lines. The ideal MHD condition readily implies that $\Omega(\Psi)$ is conserved on magnetic flux surfaces. The other quantities are conserved only when $q_n = q^{\alpha} = 0$. In the general case, the rate of change of η, $\mathcal{E}$, $\mathcal{L}$, and s along streamlines is dictated by Eqs. (3)–(6). From Ohm's law, $F_{\varphi\mu}u^{\mu} = 0$, and Eq. (4) one obtains

$$u^{\alpha}\partial_{\alpha}\eta = \frac{u_p q_n}{B_p}. \tag{11}$$

Likewise, contracting $g_{\beta\gamma}$ with Eq. (3), using the relation $(\sqrt{-g}g^{\alpha\beta})_{,\alpha} + \sqrt{-g}\Gamma^{\beta}_{\mu\nu}g^{\mu\nu} = 0$, taking the t and φ components, and noting that $\Gamma_{\mu t\nu}u^{\mu}u^{\nu} = 0$ for a stationary flow yields

$$\frac{1}{\sqrt{-g}}\partial_{\alpha}(\sqrt{-g}\epsilon^{\alpha}) = -q_t, \tag{12}$$

$$\frac{1}{\sqrt{-g}}\partial_{\alpha}(\sqrt{-g}l^{\alpha}) = q_\varphi, \tag{13}$$

where the energy and angular momentum fluxes are given by $\epsilon^{\alpha} \equiv -T^{\alpha}_{t} = \rho u^{\alpha}\mathcal{E}$ and $l^{\alpha} \equiv T^{\alpha}_{\varphi} = \rho u^{\alpha}\mathcal{L}$, respectively. Finally, the change in the entropy flux, $s^{\alpha} = (\rho/m_N)u^{\alpha}s$, where m_N is the nucleon rest mass and s denotes that dimensionless entropy per baryon, is obtained by contracting u_β with Eq. (3):

$$\frac{kT}{\sqrt{-g}}\partial_{\alpha}(\sqrt{-g}s^{\alpha}) = -u_{\alpha}q^{\alpha}. \tag{14}$$

The normalization condition $u^{\alpha}u_{\alpha} = -1$ yields the relation $1 + u_p^2 = (\alpha u^t)^2 - \varpi^2(u^\varphi - \omega u^t)^2$. By employing Eqs. (9) and (10) the latter condition can be written in the form given by Eq. (A6). Differentiating the latter equation along a given streamline yields

$$(\ln u_p)' = \frac{N}{D}, \tag{15}$$

where the prime denotes derivative along the streamline $\Psi = \text{const}$ and N and D are given explicitly in the Appendix.

B. Flow geometry

In a self-consistent treatment, the stream function $\Psi(r,\theta)$ is obtained by solving the transfield equation. Such an analysis is beyond the scope of this paper. To evaluate the conditions required for the activation of the BZ process we invoke, in what follows, a split-monopole configuration. Such a configuration can be described by a stream function of the form $\Psi(r,\theta) = \Psi_0(1 - \cos\theta)$. With this choice the redshifted poloidal field is given by $B_p = \Psi_0/(2\pi\sqrt{\Sigma\Delta})$. The poloidal velocity is given by $u_p = \sqrt{\Sigma/\Delta}u^r$, and the convective derivative reduces to $u^{\alpha}\partial_{\alpha} = u^r\partial_r = \sqrt{\Delta/\Sigma}u_p\partial_r$. The energy and angular momentum fluxes have only a radial component:

$$\epsilon^r = \rho\mathcal{E}u^r = \frac{\Psi_0}{2\pi\Sigma}\eta\mathcal{E}, \tag{16}$$

$$l^r = \rho \mathcal{L} u^r = \frac{\Psi_0}{2\pi\Sigma}\eta\mathcal{L}. \quad (17)$$

In the next section we show that the sign of the energy flux on the horizon, ϵ^r_H, or equivalently $\eta_H\mathcal{E}_H$, determines some properties of the flow.

III. TWO TYPES OF FLOWS

The nature of the flow depends on the rate at which energy (including rest mass energy) is deposited on magnetic field lines. We identify two distinct types of solutions, that correspond to regimes where the BZ process is switch on or switch off. As we now show, these two types of solutions are characterized by the sign of the specific energy $\mathcal{E}$ on the horizon.

Let $r_{\rm st}$ denotes the stagnation radius, where $u_p = \eta = 0$. Then, for the double transmagnetosonic flow considered here $\eta(r) < 0$ at $r < r_{\rm st}$ and $\eta(r) > 0$ at $r > r_{\rm st}$. Substituting Eq. (16) into Eq. (12) and integrating over r we have

$$\eta(r)\mathcal{E}(r) = \eta_H\mathcal{E}_H + \frac{2\pi}{\Psi_0}\int_{r_H}^{r}(-q_t)\Sigma dr', \quad \text{at } r < r_{\rm st}, \quad (18)$$

$$\eta(r)\mathcal{E}(r) = \eta_\infty\mathcal{E}_\infty - \frac{2\pi}{\Psi_0}\int_{r}^{r_\infty}(-q_t)\Sigma dr', \quad \text{at } r > r_{\rm st}. \quad (19)$$

The subscripts H and ∞ denote the values of quantities on the horizon and at infinity, respectively. The integrals on the right-hand side of Eqs. (18) and (19) are associated with energy injection by the external source and, therefore, must be positive. Likewise, $\mathcal{E}_\infty > 0$ always. Thus, $\eta\mathcal{E} > 0$ at $r > r_{\rm st}$ for both types of flows. Now, below we show that when $0 < \Omega_F < \Omega_H$ and the inertia of the injected matter is sufficiently low, the specific energy on the horizon is negative, $\mathcal{E}_H < 0$. In that case $\eta_H\mathcal{E}_H > 0$, and from Eq. (16) also $\epsilon^r_H > 0$, implying that energy is extracted from the black hole. From Eq. (18) it is seen that the energy flux at the stagnation radius must be finite, that is, $\eta_{\rm st}\mathcal{E}_{\rm st} > \eta_H\mathcal{E}_H > 0$. This means that the energy per baryon diverges at $r = r_{\rm st}$; specifically $\mathcal{E}(r_{\rm st} - \epsilon) \to -\infty$, and $\mathcal{E}(r_{\rm st} + \epsilon) \to +\infty$. The singularity of the specific energy at $r_{\rm st}$ is a consequence of the fact that the total energy flux there is purely electromagnetic.[1] From Eq. (A6) we have

$$\mathcal{E}_{\rm st} - \Omega_F\mathcal{L}_{\rm st} = \bar{h}_{\rm st}\sqrt{k_{\rm ost}}, \quad (20)$$

yielding $\tilde{L}_{\rm st} \equiv \mathcal{L}_{\rm st}/\mathcal{E}_{\rm st} = \Omega_F^{-1}$. The azimuthal magnetic field at $r_{\rm st}$ can be readily obtained from Eq. (9):

$$B_\varphi(r_{\rm st}) = -\frac{4\pi\eta_{\rm st}\mathcal{E}_{\rm st}}{\alpha_{\rm st}\varpi_{\rm st}\Omega_F}, \quad (21)$$

and it is seen that B_φ maintains its sign across the stagnation zone. The above considerations indicate that in this regime the dynamics of the flow is governed by the black hole rotation. In the force-free limit, in which the inertia of injected matter is negligible, that is, $2\pi\int_{r_H}^{r_\infty}(-q_t)\Sigma dr/(\Psi_0\eta_H\mathcal{E}_H) \to 0$, Eqs. (18) and (19) yield $\eta_\infty\mathcal{E}_\infty = \eta_H\mathcal{E}_H$, confirming that the spin down power of the black hole is the sole energy source of the outflow. Note that the structure of this type of flows is fundamentally different than that of an ideal MHD outflow from a stellar surface (see, e.g., [21–23]), as there is a region is space where energy is flowing against the plasma stream. This strange behavior is a unique feature of frame dragging, that allows the existence of two light surfaces: a conventional one located well outside the ergosphere and an inner one located inside the ergosphere where $g_{tt} > 0$ (see the Appendix for further details). As explained above, within the inner light surface particles must travel radially inward along negative energy trajectories.

As shown below, when loading of magnetic field lines by the external source exceeds a critical value, the specific energy on the horizon becomes positive, $\mathcal{E}_H > 0$. Then, $\eta_H\mathcal{E}_H < 0$, meaning that the black hole is fed by the external source. Since $\eta_\infty\mathcal{E}_\infty > 0$, it is evident that the energy flux changes sign in the injection zone, and so must vanish at $r_{\rm st}$; that is, $\eta_s\mathcal{E}_{\rm st} = 0$. Consequently, the specific energy is finite and continuous at $r_{\rm st}$, unlike the behavior of the previous flow type. Equation (A7) yields $B_\varphi(r_{\rm st}) = 0$, implying that B_φ must also change sign across the stagnation radius. As seen from Eqs. (18) and (19), $|\eta_\infty\mathcal{E}_\infty| + |\eta_H\mathcal{E}_H| = 2\pi\Psi_0^{-1}\int_{r_H}^{r_\infty}(-q_t)\Sigma dr$, indicating that the flow is powered by the energy deposited on magnetic field lines alone. Thus, this type of flow is driven by the external source rather than by the spin energy of the black hole. The angular velocity Ω_F is presumably fixed by the rotation of injected matter, as suggested by the fact that $B_\varphi = 0$ and $\Omega_F = v^\varphi$ at $r_{\rm st}$ [see Eq. (8)]. The properties of the outflow emanating from the stagnation radius are similar in some respects to those of outflows ejected from a stellar surface or an accretion disk. Sufficiently far out they may be well described by Michel's solution [21,22] if they are sufficiently magnetized. A particular example of such a flow with $a = \Omega_F = 0$ and a realistic energy deposition profile is outlined in [24].

IV. A CRITICAL LOAD

To simplify the analysis we suppose that the injection zone is infinitely thin, that is, $q^\alpha(r) \propto \delta(r - r_{\rm st})$, and likewise q_n. Since we are merely interested here in evaluating the dependence of the energy flux at the horizon, ϵ^r_H, on the load, it is sufficient to consider the inflow section in the region $r_H < r < r_{\rm st}$. For the injection model adopted here Eqs. (11)–(14) imply that η, $\mathcal{E}$, $\mathcal{L}$ and s are conserved on magnetic surfaces in the region $r_H < r < r_{\rm st}$. The structure

[1]This can be directly seen by applying Eq. (9) at $r_{\rm st}$ after multiplying by η, and using $\eta_{\rm st} = 0$.

of the flow is then obtained upon integration of Eq. (15). To elucidate key features, we present results obtained in two extreme limits: a cold flow and a relativistically hot flow.

A. Cold flow

We consider first a cold adiabatic flow. We set $\bar{h} = 1$ and note that in the absence of plasma injection ($q^\alpha = q_n = 0$) the location of the slow magnetosonic point of a cold flow, $r_{\rm sm}$, coincides with the stagnation radius, that is, $u_p(r_{\rm sm}) = u_{\rm sm} = 0$. As argued by [8], the requirement that u_p' remains finite at the slow point, where $D = 0$, implies $k_0' = 0$ there. This can be readily verified by taking the limit $a_s^2 \to 0$, $u_p \to u_{\rm sm}$ in Eqs. (A8)–(A16). For the split-monopole geometry adapted here this condition reads

$$\frac{d}{dr}[\alpha^2 - \varpi^2(\Omega_F - \omega)^2] = 0. \tag{22}$$

The solution of the latter equation gives the slow magnetosonic radius on every streamline, $r_{\rm sm}(\theta)$. In general, the stagnation radius $r_{\rm st}$ does not coincide with $r_{\rm sm}$, meaning that the slow point is located inside the injection zone, where the above analysis breaks down. Moreover, the exact shape of magnetic surfaces should depend on the details of the plasma injection process (although we anticipate small deviations from the split-monopole configuration adopted here in the regime of small inertia). In the following, we ignore these complications and restrict our analysis to radial inflows. We note that for every choice of η, Ω_F and θ there exists a unique solution outside the injection zone, in the region $r_H < r < r_{\rm st}$, that passes smoothly through the fast magnetosonic point. Each such solution can be extrapolated to the radius $r_{\rm sm} > r_{\rm st}$ where the boundary condition $u_p = 0$ can be used. This procedure is not mandatory and has been used for convenience. The value of η at $r = r_{\rm st} - \epsilon$ depends on the particle source q_n; for $q_n(r) = q_{n0}\delta(r - r_{\rm st})$ we obtain from Eq. (11)

$$\eta = \frac{q_{n0}}{B_{p\rm st}}\sqrt{\Sigma_{\rm st}/\Delta_{\rm st}}. \tag{23}$$

The implicit assumption underlining our analysis is that the acceleration of the flow within the injection zone is consistent with the boundary conditions at $r_{\rm st}$. For our simple injection model this condition can be fulfilled for appropriate choice of the source terms q^α. Self-consistent calculations of double transmagnetosonic flows with realistic injection profiles will be presented in a followup paper.

We seek solutions that describe an inflow of plasma into the black hole ($u_p \le 0$). For a given choice of the black hole parameters a and m, magnetic flux Ψ_0, and angular velocity Ω_F, this family of solutions is characterized by η and θ. For a given choice of η, a solution is obtained by integrating Eq. (15) along a streamline defined by $\theta = \theta_0$. The integration starts at $r_{\rm sm}(\theta_0)$, which we compute first using Eq. (22), and is repeated iteratively by changing the value of $\mathcal{E}$ until a smooth transition across the fast magnetosonic point is achieved. The value of $\tilde{L}$ is computed, in every run, from Eq. (20). A typical negative energy inflow solution, computed using $\eta = 0.023\ {\rm g\,cm^{-2}\,s^{-1}\,G^{-1}}$, $a/m = 0.95$, $\Omega_F = \Omega_H/2$, $\theta_0 = 90°$, is displayed in Fig. 2 (solid line). It starts from the slow magnetosonic radius ($r_{\rm sm} = 2.75m$), denoted SMP in the figure, and passes through the Alfvén and the fast magnetosonic points, denoted AP and FMP, respectively.

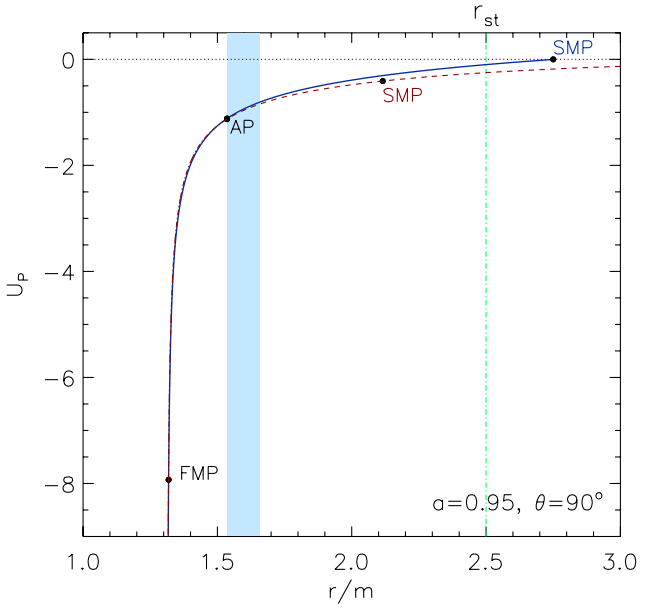

FIG. 2 (color online). Radial profiles of the poloidal velocity u_p of a cold (solid line) and a relativistically hot (dashed line) negative energy flow with a radial magnetic field. The slow-magnetosonic, Alfvén, and fast-magnetosonic points are indicated by SMP, AP, and FMP, respectively. The fast-magnetosonic point of the hot flow is located at ($r/m = 1.315$, $u_p = -11.53$) and is not shown. The stagnation radius $r_{\rm st}$ is marked by the vertical dotted-dashed line. The blue shaded region delineates the permitted range of Alfvén radii of all negative energy solutions.

Figure 3 delineates the dependence of $\eta\mathcal{E}$ on the mass-to-magnetic flux ratio η in the regime where energy extraction is switched on ($\mathcal{E} < 0$), for different values of a and θ. For convenience, we give also the values of the angular distribution of the mass flow rate and extracted power, defined here as

$$\dot{\mathcal{M}}(\theta) = 2\pi\Sigma\rho u^r = \eta\Psi_0 \tag{24}$$

and

$$P(\theta) = 2\pi\Sigma\epsilon^r = \dot{\mathcal{M}}\mathcal{E}, \tag{25}$$

respectively. The horizontal dashed lines mark the analytic result derived by BZ in the force-free limit for $\Omega_F = \Omega_H/2$:

$$P_{\rm FF}(a,\theta) = \frac{c}{128\pi^2}\left(\frac{a}{m}\right)^2\frac{(r_H^2 + a^2)\sin^2\theta}{r_H^2(r_H^2 + a^2\cos^2\theta)}\Psi_0^2, \tag{26}$$

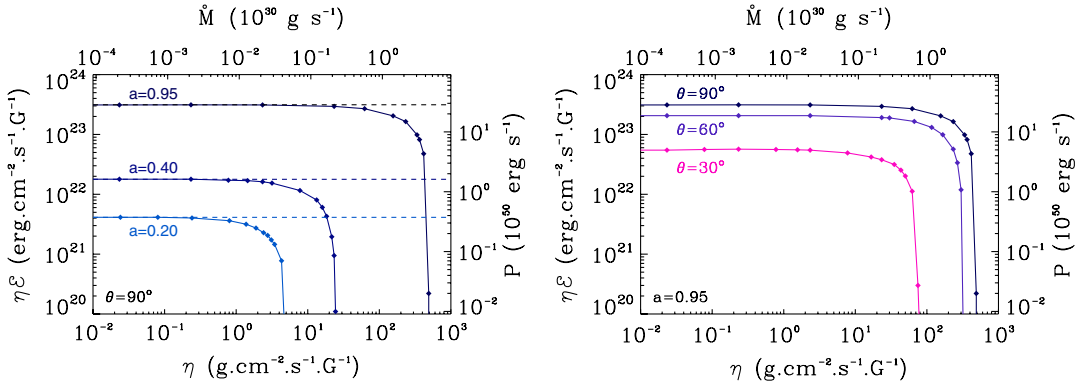

FIG. 3 (color online). Total energy flux $\eta\mathcal{E}$ vs mass-to-magnetic flux ratio η, in the regime where energy extraction is switched on. Each point corresponds to a cold, negative energy solution, like the example shown in Fig. 2. The values of the mass flux $\dot{\mathcal{M}}(\theta)$ and power $P(\theta)$, defined in Eqs. (24) and (25), are given in the top and right axis, respectively, for $\Psi_0 \approx 9 \times 10^{27}$ G cm^2. The horizontal dashed lines shown in the left panel correspond to the BZ power of a force-free flow, given explicitly in Eq. (26).

and it is seen that the extracted power converges to this limit at sufficiently small loads but is strongly suppressed as the load approaches the critical value $\dot{\mathcal{M}}_c = P_{\rm FF}/c^2$ (or $\eta_c = P_{\rm FF}/\Psi_0$), and eventually switched off.

In order to compare our result with the test simulations of [7], we employ Eqs. (24) and (26) to write

$$\frac{P_{\rm FF}}{\dot{\mathcal{M}}c^2} = \frac{(r_H^2 + a^2)\sin^2\theta}{8(r_H^2 + a^2\cos^2\theta)}\kappa^2, \tag{27}$$

where κ is the parameter defined in Eq. (6) of [7]. From Fig. 3 we find the activation condition to be $P_{\rm FF}/\dot{\mathcal{M}}c^2 > 0.5$ on the equatorial plane for $a = 0.95$, which corresponds to $\kappa > 2$, in a good agreement with [7].

B. Hot flow

Next, we generalize the above analysis to a hot flow $\bar{h} > 1$. We assume that the pressure p is dominated by radiation and set $w = \rho\bar{h} = \rho + 4p$. Unlike in the case of a cold inflow, the slow magnetosonic point of a hot inflow is located below the stagnation radius, at $r_{\rm sm} < r_{\rm st}$, and is unknown *a priori*. Thus, our strategy is to start the integration of Eq. (15) at some radius below $r_{\rm sm}$ and seek solutions that pass smoothly through both the slow-and-fast magnetosonic points. A typical negative energy, hot inflow solution is delineated by the dashed line in Fig. 2. The family of solutions thereby computed is characterized by the parameter $(wu_p/B_p)_{\rm sm}$, that denotes the enthalpy flux per unit magnetic flux at the slow magnetosonic point, and which reduces to η at zero temperature. In the spirit of Eq. (24) we define the quantity

$$\dot{w}_{\rm sm}(\theta) = \Psi_0(wu_p/B_p)_{\rm sm} = (2\pi\Sigma wu^r)_{\rm sm}, \tag{28}$$

which approaches $\dot{\mathcal{M}}(\theta)$ in the limit $\bar{h} \to 1$. As shown in Fig. 3, the effect of the load on the extracted power can be quantified in terms of this parameter.

The specific entropy of a relativistically hot gas is given approximately by $s = w/(nkT)$. Substituting the latter relation into Eq. (14) and adopting for simplicity $q^\alpha = \dot{Q}_0\delta(r - r_{\rm st})[1, 0, 0, 0]$, we obtain $(wu^r)_{\rm st} \simeq \gamma_{\rm st}\dot{Q}_0$. Since the enthalpy flow rate $2\pi\Sigma wu^r$ barely changes along streamlines, and since $\gamma_{\rm st} \simeq 1$, we have approximately

$$\dot{w}_{\rm sm} \simeq 2\pi\Sigma_{\rm st}\dot{Q}_0 \simeq P_{\rm inj}(\theta), \tag{29}$$

where $P_{\rm inj}(\theta) = d\dot{E}_{\rm ext}/d(\cos\theta)$ denotes the angular distribution of the power deposited in the magnetosphere by the external energy source.

Figure 4 exhibits the dependance of the outgoing energy flux $\eta\mathcal{E}$ on $(wu_p/B_p)_{\rm sm}$ for $\theta = \pi/2$ and different values of a. As seen from the figure, the critical condition for activation of the BZ process is $\dot{w}_{\rm sm} < P_{\rm FF}$ or, using Eq. (29), $P_{\rm inj}(\theta) < P_{\rm FF}(a, \theta)$. This condition generalizes

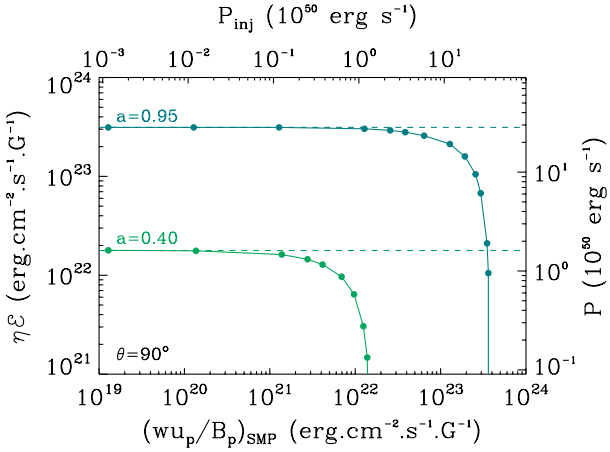

FIG. 4 (color online). Dependence of $\eta\mathcal{E}$ on the enthalpy flux per unit magnetic flux at the slow magnetosonic point, $(wu_p/B_p)_{\rm sm}$, computed for a family of relativistically hot, negative energy solutions. The upper axis gives the injected power, Eq. (29), and the right axis the extracted power defined in Eq. (25).

the cold flow result, for which $P_{\rm inj} = \dot{\mathcal{M}}c^2$, to a flow with arbitrary temperature.

V. DISCUSSION

The above results indicate that the rotational energy of a Kerr black hole can be magnetically extracted provided that the rate at which energy is deposited on magnetic field lines by the plasma source does not exceed the BZ power of a force-free flow, given explicitly in Eq. (26). In the case of a cold plasma, this condition reduces to a limit on the mass flux flowing into the black hole along a magnetic surface. When expressed in terms of the angular distribution of the mass flow rate, $\dot{\mathcal{M}}(\theta) = d\dot{M}/d(\cos\theta)$, this critical condition reads

$$\dot{\mathcal{M}}(\theta) < 10^{-4}\left(\frac{M_{\rm BH}}{3M_\odot}\right)^{-2}\left(\frac{\Psi_0}{10^{27}\,{\rm G\,cm^2}}\right)^2 g(a,\theta)\,{\rm M_\odot\,s^{-1}}, \quad (30)$$

where $g(a,\theta) = a^2(r_H^2 + a^2)\sin^2\theta/[r_H^2(r_H^2 + a^2\cos^2\theta)]$.

A rough estimate of the maximum magnetic flux that can be accumulated near the horizon of the black hole in a GRB engine can be obtained using the disk model of [10], and assuming equipartition of gas and magnetic pressure:

$$\Psi_{\rm max} \simeq 10^{29}\left(\frac{\alpha_{\rm viss}}{0.1}\right)^{-0.55}\left(\frac{M_{\rm BH}}{3M_\odot}\right)^{1.05}\left(\frac{\dot{M}_{\rm acc}}{M_\odot s^{-1}}\right)^{0.5}\,{\rm G\,cm^2}, \quad (31)$$

where $\alpha_{\rm viss}$ and $\dot{M}_{\rm acc}$ denote the viscosity parameter and accretion rate of the neutrino-cooled accretion flow, respectively. Equation (31) largely overestimates the actual value of the flux that is likely to be accumulated. Firstly, more realistic disk models [25] yield a smaller pressure in the inner disk regions and, hence, smaller $\Psi_{\rm max}$, by about an order of magnitude. Secondly, only some fraction of this maximum value is accumulated in practice. We anticipate $\Psi_0 \lesssim 10^{28}\,{\rm G\,cm^2}$ even at accretion rates approaching $\sim 1\,{\rm M_\odot\,s^{-1}}$. This implies that along field lines that extract energy from the black hole, mass inflow must be strongly suppressed. Suppression of the baryon load is expected in the polar region by virtue of the angular momentum barrier. But even then, the requirements for energy extraction and formation of a relativistic outflow impose stringent constraints on the progenitors, as discussed in [7].

Another plasma source in GRB jets is annihilation of MeV neutrinos that emanate from the hyperaccretion disk surrounding the black hole. The plasma thereby deposited is relativistically hot, and so a polar outflow will be driven either by the black hole or by the pressure of the injected plasma, provided that the central region is baryon poor, as explained above. The type of the outflow will be determined by the energy load of magnetic field lines, as explained in Sec. III. Detailed calculations that exploit an advanced disk model [12] yield a net energy deposition rate of $\dot{E}_{\nu\bar{\nu}} \simeq 10^{52}\dot{m}_{\rm acc}^{9/4}(\frac{M_{\rm BH}}{3M_\odot})^{-3/2}x_{\rm mso}^{-4.8}\,{\rm erg\,s^{-1}}$, for accretion rates (henceforth measured in units of $M_\odot\,{\rm s^{-1}}$) in the range $\dot{m}_{ign} < \dot{m}_{\rm acc} < \dot{m}_{\rm trap}$, where $x_{\rm mso}$ is the radius of marginally stable orbit in units of m. Assuming for simplicity a uniform angular distribution, viz., $P_{\rm inj}(\theta) = \dot{E}_{\nu\bar{\nu}}/2$, we derive an approximate condition for activation of the BZ process:

$$\dot{m}_{\rm acc} < 0.1\left(\frac{M_{\rm BH}}{3M_\odot}\right)^{-2/9}\left(\frac{\Psi_0}{10^{27}\,{\rm G\,cm^2}}\right)^{8/9} f(a,\theta). \quad (32)$$

The function $f(a,\theta)$ satisfies $f(0,\theta) = 0$, but otherwise depends weakly on a. For $\theta = \pi/2$ it varies between 1 and 1.2 in the range $0.95 \geq a \geq 0.2$. When condition (32) is satisfied, the outflow is powered by the spinning black hole. When this condition is violated, the flow is driven by the pressure of the $e^{\pm}$ pairs produced in the magnetosphere. In the latter case, a fraction of the injected power will emerge at infinity in the form of a relativistic outflow, and the rest will get absorbed by the black hole. A particular example of such a double-transonic flow is exhibited in [24].

The relatively sensitive dependence of the switch-on condition on black hole spin (see Fig. 3) suggests that slowly rotating black holes in AGNs (and perhaps also in x-ray binaries) are either quiet, or have underpowered outflows. For instance, if the black hole is surrounded by a thick disk, then it could be that the inclination angles of magnetic field lines that have a sufficiently low mass load to allow energy extraction depend on the angular momentum of the hole a via the activation condition (30). This may result in a steeper dependence of the jet power on a than the usual scaling obtained in the force-free limit, and may explain the claimed radio loud and quiet dichotomy [13]. A different, though perhaps related, explanation for this dichotomy has been offered by [26].

APPENDIX: DERIVATION OF THE EQUATION OF MOTION OF THE MHD FLOW

Defining M as the poloidal Alfvénic Mach number through $M^2 \equiv 4\pi\bar{h}\eta^2c^2/\rho = u_p^2/u_A^2$, where $u_A^2 = B_p^2/(4\pi\bar{h}\rho c^2)$, and given the following expressions:

$$k_0 = \alpha^2 - \varpi^2(\Omega_F - \omega)^2, \quad (A1)$$

$$k_2 = (\mathcal{E} - \Omega_F\mathcal{L})^2, \quad (A2)$$

$$k_4 = \frac{\mathcal{L}^2}{\varpi^2} - \frac{(\mathcal{E} - \omega\mathcal{L})^2}{\alpha^2}, \quad (A3)$$

we can use the constants of motion (7)–(10) and the normalization condition of the 4-velocity, $u^\alpha u_\alpha = -1$, to obtain algebraic relations for the 4-velocity components:

$$u^t = \frac{\alpha^2(\mathcal{E} - \Omega_F\mathcal{L}) - M^2(\mathcal{E} - \omega\mathcal{L})}{\alpha^2\bar{h}(k_0 - M^2)}, \quad (A4)$$

$$u^\varphi = \frac{\alpha^2\Omega_F(\mathcal{E} - \Omega_F\mathcal{L}) - M^2\omega(\mathcal{E} - \omega\mathcal{L}) - M^2L\alpha^2\varpi^{-2}}{\alpha^2\bar{h}(k_0 - M^2)}, \quad (A5)$$

$$u_p^2 + 1 = \frac{k_2(k_0 - 2M^2) - k_4 M^4}{\bar{h}^2(k_0 - M^2)^2}. \tag{A6}$$

We also express the toroidal component of the magnetic field as

$$B_\varphi = -\frac{4\pi\eta}{\alpha\varpi}\frac{\alpha^2\mathcal{L} - \varpi^2(\Omega_F - \omega)(\mathcal{E} - \mathcal{L}\omega)}{k_0 - M^2}. \tag{A7}$$

Equation (A6) is the wind equation for the poloidal velocity [8,18]. Upon differentiating this equation along a given streamline $\Psi = \text{const}$, one obtains the equation of motion

$$(\ln u_p)' = \frac{N}{D}, \tag{A8}$$

with

$$N = \zeta_1(\ln B_p)' + \zeta_2(\ln\alpha)' + \zeta_3(\ln\varpi)' + \zeta_4(\ln\mathcal{E})' + \zeta_5(\ln s)' + \zeta_6(\ln\omega)', \tag{A9}$$

$$D = (k_0 - M^2)^2\left[(u_p^2 - c_s^2)(k_0 - M^2) + \frac{M^4}{\bar{h}^2}\frac{(k_0 k_4 + k_2)}{(k_0 - M^2)^2}\right]. \tag{A10}$$

Here c_s^2 is the sound 4-velocity defined by $c_s^2 = a_s^2/(1 - a_s^2)$, with a_s^2 is given by Eq. (25) in [27], and

$$\zeta_1 = -(k_0 - M^2)^2\left[(1 + u_p^2)(k_0 - M^2)c_s^2 - M^2\frac{B_\varphi^2}{4\pi\bar{h}\rho}\right], \tag{A11}$$

$$\zeta_2 = \frac{1}{\bar{h}^2(1 - a_s^2)}\left\{\frac{M^6(\mathcal{E} - \omega\mathcal{L})^2}{\alpha^2} - \left[(\mathcal{E} - \omega\mathcal{L})^2\left(3 - \frac{\varpi^2\delta\Omega^2}{\alpha^2}\right) - \frac{2\alpha^2\mathcal{L}^2}{\varpi^2}\right]M^4 + \alpha^2 k_2(3M^2 - k_0)\right\}, \tag{A12}$$

$$\zeta_3 = \frac{1}{\bar{h}^2(1 - a_s^2)}\left\{-\frac{M^6\mathcal{L}^2}{\varpi^2} - \left[3\mathcal{L}^2\delta\Omega^2 - \frac{\alpha^2\mathcal{L}^2}{\varpi^2} - \frac{2\varpi^2}{\alpha^2}\delta\Omega^2(\mathcal{E} - \omega\mathcal{L})^2\right]M^4 - \varpi^2\delta\Omega^2 k_2(3M^2 - k_0)\right\}, \tag{A13}$$

$$\zeta_4 = \frac{1}{\bar{h}^2(1 - a_s^2)}(k_0 - M^2)\left[(k_0 - 2M^2)(\mathcal{E} - \Omega_F\mathcal{L})\mathcal{E} + \frac{M^4\mathcal{E}}{\alpha^2}(\mathcal{E} - \omega\mathcal{L})\right], \tag{A14}$$

$$\zeta_5 = \frac{s c_s^2(5 + 8\sigma)}{\bar{h}^2(5 + 10\sigma + 2\sigma^2)}[-k_4 M^6 - k_2(k_0^2 - 3k_0 M^2 + 3M^4)], \tag{A15}$$

$$\zeta_6 = -\frac{1}{\bar{h}^2(1 - a_s^2)}\left[M^4(k_0 - M^2)(\mathcal{E} - \omega\mathcal{L})\frac{\mathcal{L}\omega}{\alpha^2} + \varpi^2\omega\delta\Omega(k_0 k_2 - 3k_2 M^2 - 2k_4 M^4)\right] \tag{A16}$$

generalize the coefficients $\zeta_{i=1,6}$ derived in [27] in the Schwarzschild geometry, where for short we denote $\delta\Omega \equiv \Omega_F - \omega$.

1. Critical surfaces

The requirement of a smooth transition between the sub- and super-Alfvénic regimes yields the following regularity condition at the Alfvén surface, where the denominator of Eqs. (A4)–(A7) vanishes:

$$M_A^2 = \alpha_A^2 - \varpi_A^2(\Omega_F - \omega_A)^2, \tag{A17}$$

$$\varpi_A^2 = \frac{\alpha_A^2\tilde{L}}{(\Omega_F - \omega_A)(1 - \omega_A\tilde{L})}, \tag{A18}$$

where $\tilde{L} = \mathcal{L}/\mathcal{E}$. Equation (A17) has two roots that define the inner and outer Alfvén surfaces. Those surfaces approach the light surfaces in the limit of zero inertia, at which $M_A^2 \to 0$. The outer light surface is located well outside the ergosphere, where gravity is weak and to a good approximation $\alpha \simeq 1$, $\omega = 0$. To lowest order it coincides with the conventional light cylinder, $\varpi_c \simeq \Omega_F^{-1}$, as originally derived in Ref. [21] for pulsar winds. Recalling that $g_{tt} = -\alpha^2 + \varpi^2\omega^2$, and using Eq. (A17) with $M_A = 0$, gives $\varpi^2\omega^2 > g_{tt} = \varpi^2[\omega^2 - (\Omega_F - \omega)^2] > 0$ at the inner light surface. Hence, it must be located inside the ergosphere, but above the horizon since $\Omega_F < \omega_H$.

There are two additional critical surfaces, the fast-and-slow magnetosonic surfaces. Those can be most conveniently identified by expressing the denominator D [Eq. (A10)] in the form

$$D = -(k_0 - M^2)^2(u_p^2 - u_{\rm sm}^2)(u_p^2 - u_{\rm fm}^2)(u_A^2)^{-1}, \tag{A19}$$

in terms of the slow and fast magnetosonic speeds,

$$u_{\rm sm}^2 = K - \sqrt{K^2 - c_s^2 u_A^2 k_0}, \tag{A20}$$

$$u_{\rm fm}^2 = K + \sqrt{K^2 - c_s^2 u_A^2 k_0}, \tag{A21}$$

where

$$K = \frac{1}{2}\left[k_0 u_A^2 + c_s^2 + \frac{B_\varphi^2}{4\pi\bar{h}\rho}\right]. \tag{A22}$$

[1] R. D. Blandford and R. L. Znajek, Mon. Not. R. Astron. Soc. **179**, 433 (1977).
[2] S. Komissarov, Mon. Not. R. Astron. Soc. **350**, 1431 (2004).
[3] S. Hirose, J. H. Krolik, J. De Villiers, and J. Hawley, Astrophys. J. **606**, 1083 (2004).
[4] J. C. McKinney and C. F. Gammie, Astrophys. J. **611**, 977 (2004).
[5] J. C. McKinney, Astrophys. J. **630**, L5 (2005).
[6] M. Barkov and S. Komissarov, Mon. Not. R. Astron. Soc. **385**, L28 (2008).
[7] S. Komissarov and M. Barkov, Mon. Not. R. Astron. Soc. **397**, 1153 (2009).
[8] M. Takahashi, S. Nitta, Y. Tatematsu, and A. Tomimatsu, Astrophys. J. **363**, 206 (1990).
[9] M. Jaroszynski, Astron. Astrophys. **305**, 839 (1996).
[10] R. Popham, S. E. Woosley, and C. Fryer, Astrophys. J. **518**, 356 (1999).
[11] R. Birkl, M. A. Aloy, H.-Th. Janka, and E. Muller, Astron. Astrophys. **463**, 51 (2007).
[12] I. Zalamea and A. Beloborodov, Mon. Not. R. Astron. Soc. **410**, 2302 (2011).
[13] M. Sikora, L. Stawarz, and J.-P. Lasota, Astrophys. J. **658**, 815 (2007).
[14] A. Levinson, in *Trends in Black Hole Research*, edited by Paul V. Kreitler (Nova Science, New York, 2006), p. 119.
[15] A. Levinson and F. Rieger, Astrophys. J. **730**, 123 (2011).
[16] A. Levinson and D. Eichler, Astrophys. J. **594**, 19 (2003).
[17] K. S. Thorne, D. A. MacDonald, and R. H. Price, *Black Holes: The Membrane Paradigm* (Yale University, New Haven, CT, 1986).
[18] M. Camenzind, Astron. Astrophys. **162**, 32 (1986).
[19] S. Horiuchi, L. Mestel, and I. Okamoto, Mon. Not. R. Astron. Soc. **275**, 1160 (1995).
[20] M. H. P. M. van Putten and A. Levinson, *Relativistic Astrophysics of the Transient Universe* (Cambridge University Press, Cambridge, England, 2012), p. 145.
[21] F. C. Michel, Astrophys. J. **158**, 727 (1969).
[22] R. N. Henriksen and D. R. Rayburn, Mon. Not. R. Astron. Soc. **152**, 323 (1971).
[23] L. Mestel, *Stellar Magnetism* (Oxford University, New York, 2012), 2nd ed.
[24] A. Levinson and N. Globus, Astrophys. J. **770**, 159 (2013).
[25] W.-X. Chen and A. Beloborodov, Astrophys. J. **657**, 383 (2007).
[26] A. Tchekhovskoy, R. Narayan, and J. C. McKinney, Astrophys. J. **711**, 50 (2010).
[27] A. Levinson, Astrophys. J. **648**, 510 (2006).